

Confidential -28

CONF-920538--28

DE93 003549

# NEURAL NETWORKS FOR THE MONITORING OF ROTATING MACHINERY

Israel E. Alguindigue, Anna Loskiewicz-Buczak

Department of Nuclear Engineering, University of Tennessee, Knoxville, TN 37996-2300 USA

and

Robert E. Uhrig

Department of Nuclear Engineering, University of Tennessee, Knoxville, TN 37996-2300 USA

and

Instrumentation and Control Division, Oak Ridge National Laboratory, Oak Ridge, TN 37831-6005

## DISCLAIMER

This report was prepared as an account of work sponsored by an agency of the United States Government. Neither the United States Government nor any agency thereof, nor any of their employees, makes any warranty, express or implied, or assumes any legal liability or responsibility for the accuracy, completeness, or usefulness of any information, apparatus, product, or process disclosed, or represents that its use would not infringe privately owned rights. Reference herein to any specific commercial product, process, or service by trade name, trademark, manufacturer, or otherwise does not necessarily constitute or imply its endorsement, recommendation, or favoring by the United States Government or any agency thereof. The views and opinions of authors expressed herein do not necessarily state or reflect those of the United States Government or any agency thereof.

Proceedings  
of the  
8th Power Plant Dynamics, Control & Testing Symposium  
(in press)  
Knoxville, Tennessee  
May 27-29, 1992

MASTER

FC 7-581 2/2/94

DISTRIBUTION OF THIS DOCUMENT IS UNLIMITED

# **NEURAL NETWORKS FOR THE MONITORING OF ROTATING MACHINERY**

**Israel E. Alguindigue, Anna Loskiewicz-Buczak  
Robert E. Uhrig**

**The University of Tennessee  
Department of Nuclear Engineering  
Knoxville, Tennessee 37996-2300, U. S. A.**

## **ABSTRACT**

Vibration monitoring of components in engineering systems and plants involves the collection of vibration data and detailed analysis to detect features which reflect the operational state of the machinery. The analysis leads to the identification of potential failures and their causes, and makes it possible to perform efficient preventive maintenance. This paper describes a methodology for the automation of some of the activities related to motion and vibration monitoring in these systems.

The technique involves training a neural network to model the inter-relationship between signals from two related sensors mounted on an engineering system or component at a time when it is known to be operating properly. Then one signal (or its characteristics) is put into the neural network model to predict the second signal (or its characteristics). This predicted signal is continuously compared with the actual signal. A deviation between the predicted and actual signal indicates a changing relationship, usually failure of the component or system. This deviation may be quantified and provides meaningful information about the degree of degradation and deterioration of the component.

## **MONITORING OF VIBRATION SIGNATURES**

Vibration monitoring is based on the principle that all systems produce vibration during operation. When a machine is operating properly, vibration levels are generally small and constant; however, when faults develop and some of the dynamic processes in the machine change, the vibration spectrum also changes [1,2,3]. For many machines the vibration frequency spectrum has a characteristic shape when the machine is operating properly, and it has other characteristics for different faults that may appear. Monitoring can be performed effectively by close examination of the spectrum and the identification of features which are typical of particular defects; indeed, some systems have been built based on this principle [4,5,6].

The spectral features associated with particular defects of rotating machinery depend on a series of factors, among these: the kind of machine, its geometry, the operating environment and the severity of the defect. Although abundant literature (such as reference [7]) can be found which documents the vibratory behavior of rotating components, the peculiarities that need be considered for each case makes it difficult to design a general

monitoring technique applicable to a wide variety of problems. In this paper a neural network-based technique is proposed which models the relationship between sensors on a machine using actual sensor data. This technique can be used to verify the structural integrity of the vibrating component by comparing the output of one sensor with the output of other sensors at different measuring points. The comparison is useful in the identification of relevant frequencies where changes in vibration levels occur and in performing overall trend of vibration.

To implement this criterion we train a hetero-associative neural network to map the output of one sensor from the output of a different sensor. The relevance of this mapping is that while the state of operation remains unchanged, the network can make accurate predictions of the output of the sensor. However, if and when the operational state changes, the prediction of the network and the actual output of the sensor will deviate by an amount that reflects the severity of change. When it can be established that the two sensors are related in a statistical sense, the deviation may be quantified and provides important information about degradation and deterioration of the components.

To examine the properties of multiple transmission paths between a force source and different outputs, consider a one-input/two-output model (Figure 1). We assume that linear systems may be used to represent different paths and that the uncorrelated noise accounts for any significant deviations from normal cases. In the following equations  $\mathbf{x}(t)$  corresponds to the input signal,  $y_1(t)$ ,  $y_2(t)$  to the output signals and  $n_1(t)$ ,  $n_2(t)$  to the uncorrelated noise in each signal. The equations from reference [8] may be used to describe the system

$$\begin{aligned}
 G_{xn_1} &= G_{v_1n_1} = G_{xn_2} = G_{v_2n_2} = G_{n_1n_2} = 0 \\
 G_{y_1y_1} &= G_{v_1v_1} + G_{n_1n_1} = |H_1|^2 G_{xx} + G_{n_1n_1} \\
 G_{y_2y_2} &= G_{v_2v_2} + G_{n_2n_2} = |H_2|^2 G_{xx} + G_{n_2n_2}
 \end{aligned} \tag{1}$$

$$G_{xy_1} = G_{xv_1} = H_1 G_{xx} \quad G_{xy_2} = G_{xv_2} = H_2 G_{xx} \tag{2}$$

$$G_{y_1y_2} = G_{v_1v_2} = H_1^* H_2 G_{xx} \tag{3}$$

where  $G_{AB}$  is the cross-spectral density function of signals  $A(t)$  and  $B(t)$ ,  $G_{AA}$  is the power spectral density function of  $A(t)$  and  $H_i$  is the transfer function for output  $y_i(t)$ . All  $G_i$  and  $H_i$  are functions of frequency, the notation is dropped here for simplicity. The symbol '\*' indicates conjugate values.

The coherence function between the output records  $y_1(t)$ ,  $y_2(t)$  is given by

$$\begin{aligned} \gamma_{y_1 y_2}^2 &= \frac{|G_{y_1 y_2}|^2}{G_{y_1 y_1} G_{y_2 y_2}} = \frac{|G_{v_1 v_2}|^2}{G_{y_1 y_1} G_{y_2 y_2}} = \\ &= \frac{|H_1^* H_2 G_{xx}|^2 |G_{xx}|^2}{G_{y_1 y_1} G_{y_2 y_2} |G_{xx}|^2} = \frac{|H_1^2 G_{xx}^2| |H_2^2 G_{xx}^2|}{G_{xx} G_{y_1 y_1} G_{xx} G_{y_2 y_2}} = \\ &= \frac{G_{v_1 v_1} G_{v_2 v_2} G_{xx}^2}{G_{xx}^2 G_{y_1 y_1} G_{y_2 y_2}} = \frac{G_{v_1 v_1}}{G_{y_1 y_1}} \frac{G_{v_2 v_2}}{G_{y_2 y_2}} = \gamma_{xy_1}^2 \gamma_{xy_2}^2 \end{aligned} \quad (4)$$

since,

$$\begin{aligned} \gamma_{xy_1}^2 &= \frac{|G_{xy_1}|^2}{G_{xx} G_{y_1 y_1}} = \frac{|H_1 G_{xx}|^2}{G_{xx} G_{y_1 y_1}} = \frac{G_{v_1 v_1}}{G_{y_1 y_1}} \\ \gamma_{xy_2}^2 &= \frac{|G_{xy_2}|^2}{G_{xx} G_{y_2 y_2}} = \frac{|H_2 G_{xx}|^2}{G_{xx} G_{y_2 y_2}} = \frac{G_{v_2 v_2}}{G_{y_2 y_2}} \end{aligned} \quad (5)$$

When  $\gamma_{xy}^2 = 0$  at a particular frequency,  $x(t)$  and  $y(t)$  are said to be incoherent at that frequency. When  $\gamma_{xy}^2 = 1$  at all frequencies  $x(t)$  and  $y(t)$  are said to be fully coherent. So, the coherence function satisfies:

$$0 \leq \gamma_{xy}^2 \leq 1 \quad (6)$$

The coherence function will be unity for the ideal case of a constant parameter noise-free linear system with a single clearly defined input and output. When  $x(t)$  and  $y(t)$  are completely unrelated, the coherence function is zero. A value of coherence less than unity is due to noise in the measurements, non-linear relationship between the two signals or contribution of other signals to the output [8,9].

In cases where the input signal  $x(t)$  cannot be directly measured, it is possible to use Equations 1 to 5 when the transfer functions  $H_1$  and  $H_2$  are found by other methods. However, if these functions are not known, Equation 4 can be used to calculate the coherence function. A high value of the coherence function between any two output signals  $y_1(t)$  and  $y_2(t)$  indicates that  $y_1(t)$  and  $y_2(t)$  are related linearly to the input  $x(t)$  by unknown transfer functions and that the output noise is small compared to the signal [8].

When the process changes, the model no longer represents the behavior of the input/output relations and the relation between the two output signals no longer holds. Deviations from the true model can be detected and quantified if the relationship between the two outputs can be established. This relationship between  $y_1(t)$  and  $y_2(t)$  can be modeled

using a neural network which receives as input the spectrum of  $y_1(t)$  and produces as output the spectrum of  $y_2(t)$ .

This concept can be extended to the single input/multiple output system. For this system it is necessary to calculate the coherence functions between all two-signal combinations of the output records. This can be accomplished using Equation 1 through 5 where the generalized subscripts  $i$  and  $j$  are substituted for the subscripts 1 and 2. The multiple output system may provide a better diagnostic technique because different combinations of pairs of output signals may be highly coherent at different regions of the spectrum. Ideally, each frequency of the spectrum will be coherent in at least one of these combinations and the behavior of the whole spectra can be observed.

## SYSTEM DESCRIPTION

Data from the two sensors is presented to the neural network such that the input is the spectrum from one sensor and the output the spectrum from the other sensor. The network during training learns the relationship between the two sensors and is able to predict the behavior of one sensor from the other. These predictions make it possible to detect significant changes in relationship between sensor readings by comparing the actual output of the sensor with the prediction of the neural network. The changes become readily apparent when the state of the system changes because the actual value and the predicted value deviate.

Figure 2 illustrates this idea in some detail. Suppose that we are teaching the relationship between a horizontal sensor on a machine and a vertical sensor on the same machine. At an operating state A, the values of the sensors can be denoted by  $S^v_A$  (corresponding to the reading from the vertical sensor at operating state A) and  $S^h_A$  (reading from the horizontal sensor at the same operating state). Similarly, these readings may be denoted  $S^v_B$  and  $S^h_B$  when the operating state is B. If we teach the network the associations between the sensors during the A operating state when we know the machine is operating correctly (the network is trained to predict the output  $S^v_A$  from  $S^h_A$ ), recalling the network with  $S^h_B$  produces a prediction of the output of the vertical sensor,  $S^v$ , under operating condition A (lets call this prediction  $P^v_B$ ). The difference between the actual value of the sensor,  $S^v_B$ , and the predicted value,  $P^v_B$ , may be used to detect significant deviations in the signatures and to quantify this deviation.

To establish statistical relationship, we examine the value of the coherence in the whole range of frequencies of the signal. This range depends on the application; for example in the analysis of vibration signatures from rotating machinery the range of interest may be 5 Hz to 1000 Hz (base frequency) or 1 KHz to 20 KHz (high frequency), while in the context of reactor internals the range of interest is 0.5 Hz to 25 Hz [10]. In those regions of the spectrum where the coherence is high we know that there exists a linear relationship between the two output signals. This relationship is independent of the input  $x(t)$  and should remain constant while the process does not change.

Once coherent frequencies have been identified the change in vibration can be assessed by comparing the prediction of the network with the actual spectrum calculated from the sensor at the coherent frequencies. The comparison can be made using descriptors: the horizontal descriptor which gives an overall measure of vibration amplitude from the horizontal

sensor, a vertical descriptor describing the overall vibration levels in the vertical sensor. In addition, we are defining a cross-sensor descriptor which provides an overall measure of discrepancy between the two signals, and a per-frequency descriptor which represents the difference in magnitude and direction of the change in amplitude at each frequency.

The horizontal and vertical descriptors are calculated from effective velocity by integrating the output of the accelerometer in the appropriate range. The cross-sensor descriptor is a degradation indicator obtained by taking the square root of the sum of the squared differences at each frequency.

$$Cr. Desc = \sqrt{\sum_{i=1}^n (S_B^v(i) - P_B^v(i))^2} \quad (7)$$

where  $S_B^v(i)$  is the actual value, and  $P_B^v(i)$  the predicted value, both at frequency  $i$ .  $n$  is the number of frequencies in the spectrum.

The cross-sensor descriptor reflects an aspect of vibration which is critical for diagnostics: the level of disagreement among sensor outputs. This quantity would be very useful for the detection of misalignment and looseness in rotating machinery because these defects produce uneven vibration levels in the vertical and horizontal directions. Of particular importance is the fact that the cross-sensor descriptor is less sensible to wiping than the horizontal and vertical descriptors. In some cases after the component has developed a fault, the vibration descriptors calculated from independent sensor readings (vertical and horizontal in our case) return to normal levels, or even lower levels, while the value of the cross-sensor descriptor only decreases. In rolling element bearings, defects are characterized by loss of metal fragments of the cage or the rolling elements. Wiping is the process of leveling or smoothing the area surrounding a defect by the rolling elements as they pass through the defect repeatedly. The reason the descriptors return to normal or below-normal levels is smoothing which prevents the generation of sharp impulses.

The cross-sensor descriptor is able to measure the activity even if one of the sensors does not register a particular impulse since the difference among sensor readings is reflected in the measure. Another useful indicator is called the per-frequency descriptor, it gathers the differences of the amplitudes at each frequency, indicating amplitude increases or decreases. The indicator identifies the regions of the spectrum where the activity has changed and is useful in the realm of vibration since some regions of the spectrum may be mapped to certain components defects.

## TESTING ON MOTOR DATA

The monitoring system was tested on data from a motor in one of Electricite de France (EDF) operating power stations. The motor is a asynchronous horizontal electric motor (710 KW) driving a charging pump and the bearing monitored is of type NU 324 MPC3 manufactured by SKF [11]. The data was collected with two accelerometers mounted onto the machine at different measuring points - a horizontal sensor and a vertical sensor. Data from the motor was collected in 12 occasions, ranging from the normal condition of the bearing to failure due to serious cage wear. From the 12 time records collected for each sensor, high frequency spectra (1 KHz to 20 KHz) were generated. These spectra were used as input to

a neural network, which was trained to model the relationship between the spectra of the horizontal sensor and the vertical sensor mounted on the motor. In order to be able to make comparison between spectra at different times, the spectra amplitudes were normalized globally in the range 0.1 to 0.9. The first six spectra represent normal operation, the remaining signatures describe the behavior of the motor as it deteriorates.

The predicting network is a backpropagation network with 264 nodes in the input layer, 60 nodes in the first hidden layer, 30 units in the second hidden layer and 132 nodes in the output layer (Figure 3). The first 132 input nodes correspond to the spectrum from the horizontal sensor at time  $t-1$ , the next 132 input nodes correspond to the spectrum of the horizontal sensor at time  $t$ , and the output nodes correspond to the spectrum of the vertical sensor at time  $t$ . Both input spectra (time  $t$  and time  $t-1$ ) are used to account for the dynamic nature of the system. The training was performed using three pairs of normal signatures (1-2, 3-4, 5-6) and the recall was performed on all the pairs.

Figure 4 illustrates the agreement between the actual and predicted vertical sensors for a normal signature included in the training set. Figure 5 shows the agreement between the two spectra for a normal signature not included in the training set. As can be observed, the neural network has learned the relationship between the spectra of the two signals and is able to predict accurately the spectra of the vertical sensor even when the vibration increases. During monitoring it is common to observe increases in vibration while the machine is still operating under normal conditions. The network is able to adjust to this increases and to continue modeling the relationship. As a result, the prediction is not based on a single baseline signature but on a collection of signatures representing normal operations.

Figure 6 depicts the significant deviation between the actual and predicted vertical components for Signature 7; this signature describes the condition of the machine prior to the failure but after the descriptors had commenced to increase. Figure 7 depicts the contrast between the predicted value and the actual value of the sensor for Signature 12. The machine was determined to be non-functional at this point. The predicted levels of the vertical sensor (i.e. value if the machine had been working correctly) are much lower than the actual levels calculated from the sensor. Figure 8 shows the plot of the per-frequency descriptor of Signature 12. Negative values indicate decrease in vibration and positive values indicate increases.

Table 1 displays the horizontal, vertical and cross-sensor descriptors for the signatures in the recall set. The cross-sensor descriptor is sensitive to increases in vibration levels and the level of disagreement between the two sensors. A good example of wiping is Signature 11, it can be observed that the vibration level registered by the horizontal and vertical sensors are lower than those for a normal signature (Signature 2 for example) and well below the alarm criteria established by the utility. This is due to smoothing of the cage surface surrounding the defect. The cross-sensor descriptor for that signature decreases but remains close to the upper bound of normal limits.

Values of the cross-sensor descriptor may also be used to define alarm criteria based on the relationship between the sensors. In order to establish this criteria, it would be necessary to perform the analysis on baseline data and define an alarm threshold based on the calculated value of the cross-sensor descriptor for the baseline data.

	Horizontal Desc.	Vertical Desc.	Cross-Sensor Desc.
Signature 2	2.89	2.94	0.1119
Signature 3	1.80	2.31	0.2683
Signature 4	1.72	1.61	0.0878
Signature 5	1.61	1.89	0.1416
Signature 6	1.74	1.73	0.0735
Signature 7	5.31	4.97	0.9457
Signature 8	7.03	5.16	0.7148
Signature 9	5.84	5.03	0.8772
Signature 10	2.42	2.53	0.2907
Signature 11	1.55	1.48	0.2254
Signature 12	10.50	8.70	2.1101

**Table 1. Degradation Descriptors (High Freq.)**

## CONCLUSIONS

We are working on the implementation of a methodology for the analysis of vibration data based on neural networks. The anticipated advantage of developing such a system is the possibility of automating the monitoring and diagnostic process for vibrating components and building diagnostic systems which complement traditional PSD analysis.

In this paper we have proposed a methodology for the monitoring of machinery vibration based on multiple sensor modeling. A neural network has been trained to mimic the relationship among sensors in a component, and deviations from normal behavior can be detected easily by monitoring the predictions of the network and the actual values of the sensors. In addition, two descriptors are defined: the cross-sensor descriptor which measures the overall difference between the actual vibration levels and the predicted levels, and the per-frequency descriptor which gives a measure of change for every frequency in the spectrum. The methodology has been tested on data from a motor in one of EDF's power stations and has been adapted to the realm of nuclear reactor structural vibrations. In this case, the network is trained with data from ex-core neutron noise detectors in the reactor core and used to detect vibration and motion of the internals.



## REFERENCES

1. J. T. BROCH, Mechanical Vibrations and Shock Measurements, Bruel & Kjaer, 1984.
2. J. MOREL, D. LE REVERED, P. NEAU, "Vibration Monitoring of Heavy Duty Machines," Proceedings of the 4th Incipient Failure Detection Conference, Philadelphia, Pennsylvania, Oct. 1990.
3. L. WINN, "Reliability and Failure Detection of Rolling Element Bearings in Power Plant Machinery: A Utility Survey," Proceedings of the 4th Incipient Failure Detection Conference, Philadelphia, Pennsylvania, Oct. 1990.
4. I. E. ALGUINDIGUE, A. LOSKIEWICZ-BUCZAK, R. E. UHRIG, L. HAMON, F. LEFEVRE, "Vibration Monitoring of EDF Rotating Machinery Using Artificial Neural Networks," Proceedings of the AI91 Frontiers in Innovative Computing for the Nuclear Industry Conference, Jackson, Wyoming, September 15-18, 1991.
5. I. E. ALGUINDIGUE, R. E. UHRIG, "Vibration Monitoring with Artificial Neural Networks," Proceedings of the SMORN VI Symposium on Nuclear Reactor Surveillance and Diagnostics, Gatlinburg, Tennessee, May 19-24, 1991.
6. G. ZWINGELSTEIN, M. H. MASSON, B. DUBUISSON, M. PAVARD, J. M. MAZALERAT, "The Application of Neural Networks for the Predictive Maintenance of Nuclear Power Plants," Proceedings of the 3rd Symposium on Expert System Applications to Power Systems, Tokyo, Japan, April 1-5, 1991.
7. M. ANGELO, Bruel & Kjaer Technical Review: Vibration Monitoring of Machines, No.1, Naerum Offset, Denmark, 1987.
8. J. S. BENDAT, Non-Linear System Analysis and Identification from Random Data, John Wiley & Sons, New York, 1990.
9. J. S. BENDAT, A. G. PIERSOL, Random Data Analysis and Measurement Procedures, John Wiley & Sons, Second Edition, New York, 1986.
10. A. TRENTY, C. PUYAL, H. KLAJNMIC, "SINBAD, a Database for PWR Internals Vibratory Monitoring," Proceedings of the SMORN VI Symposium on Nuclear Reactor Surveillance and Diagnostics, Gatlinburg, Tennessee, May 19-24, 1991.
11. G. ZWINGELSTEIN, L. HAMON, "EDF Studies on the Condition Monitoring of Rolling Element Bearings," Proceedings of the 4th Incipient Failure Detection Conference, Philadelphia, Pennsylvania, Oct. 1990.

## ACKNOWLEDGMENT

The authors wish to acknowledge the financial contribution of Electricite de France for this project.

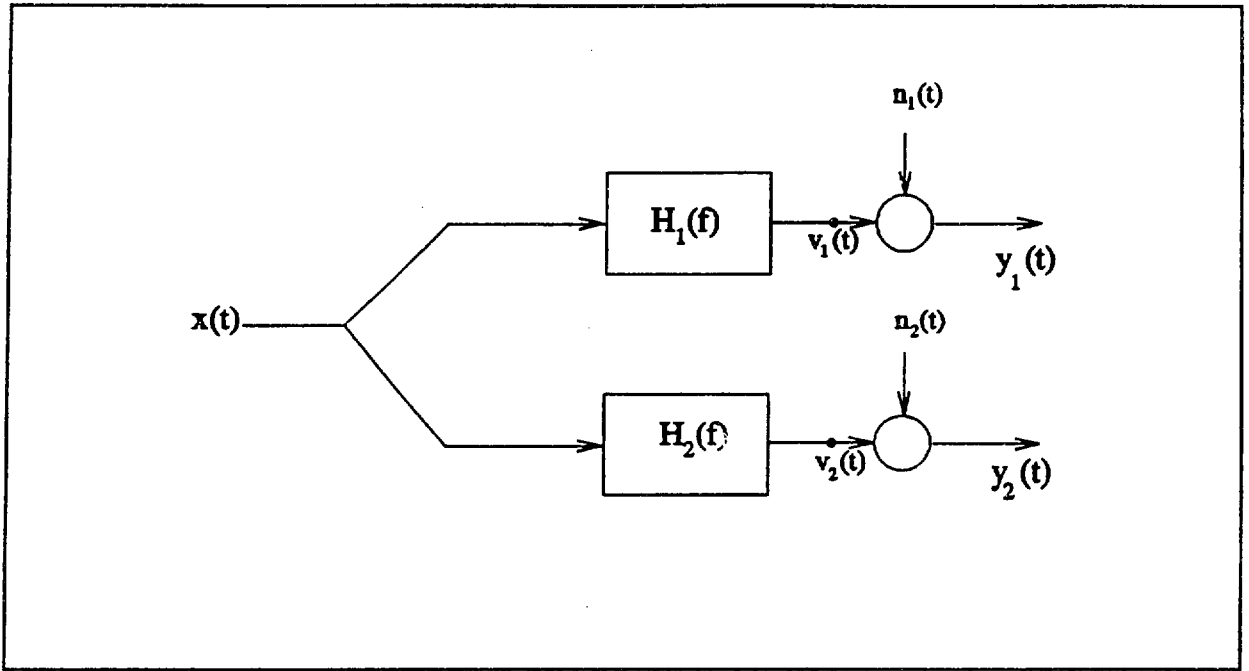


Figure 1. One Input/Two Output System

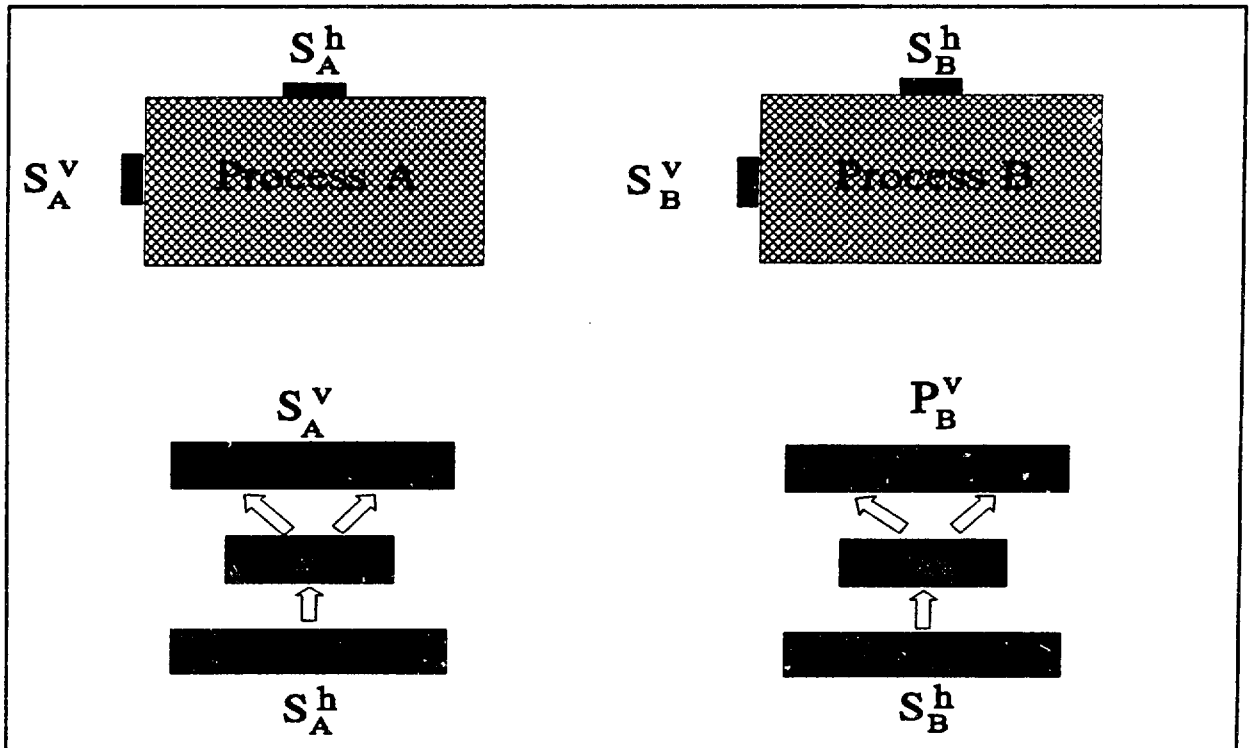


Figure 2. Prediction System Set-Up

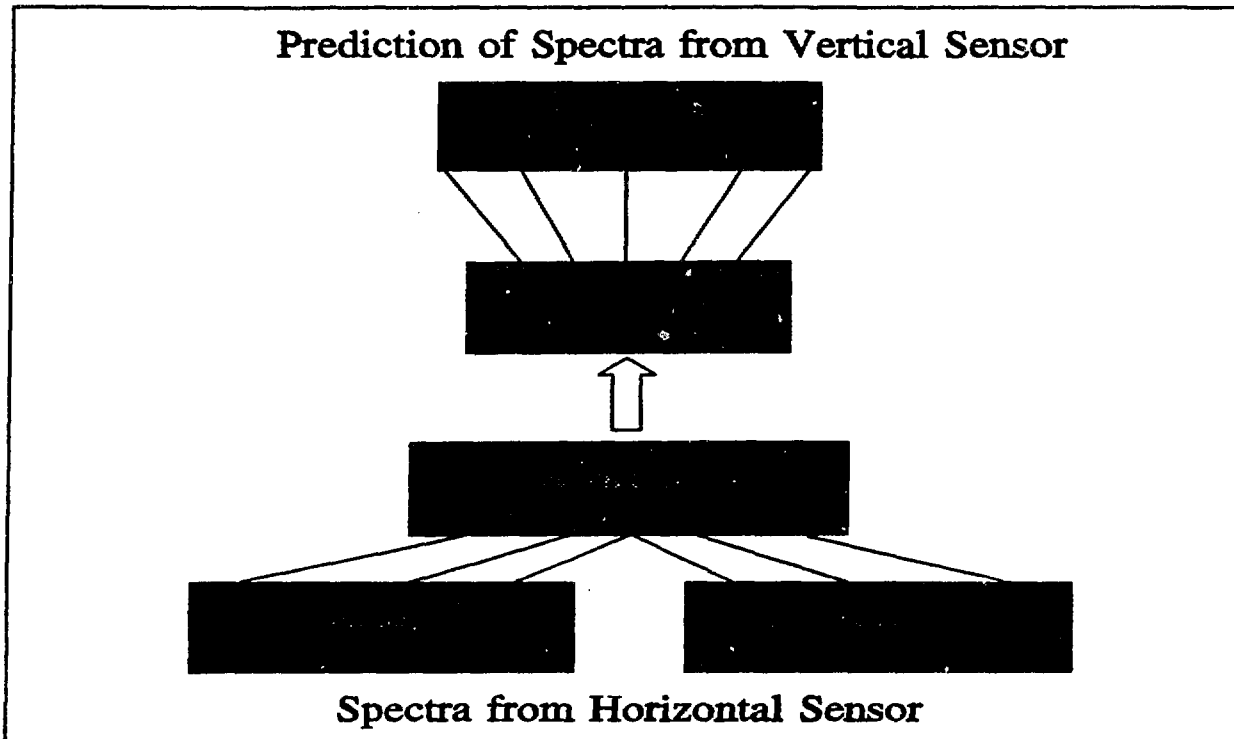


Figure 3. Topology of the Predicting Network

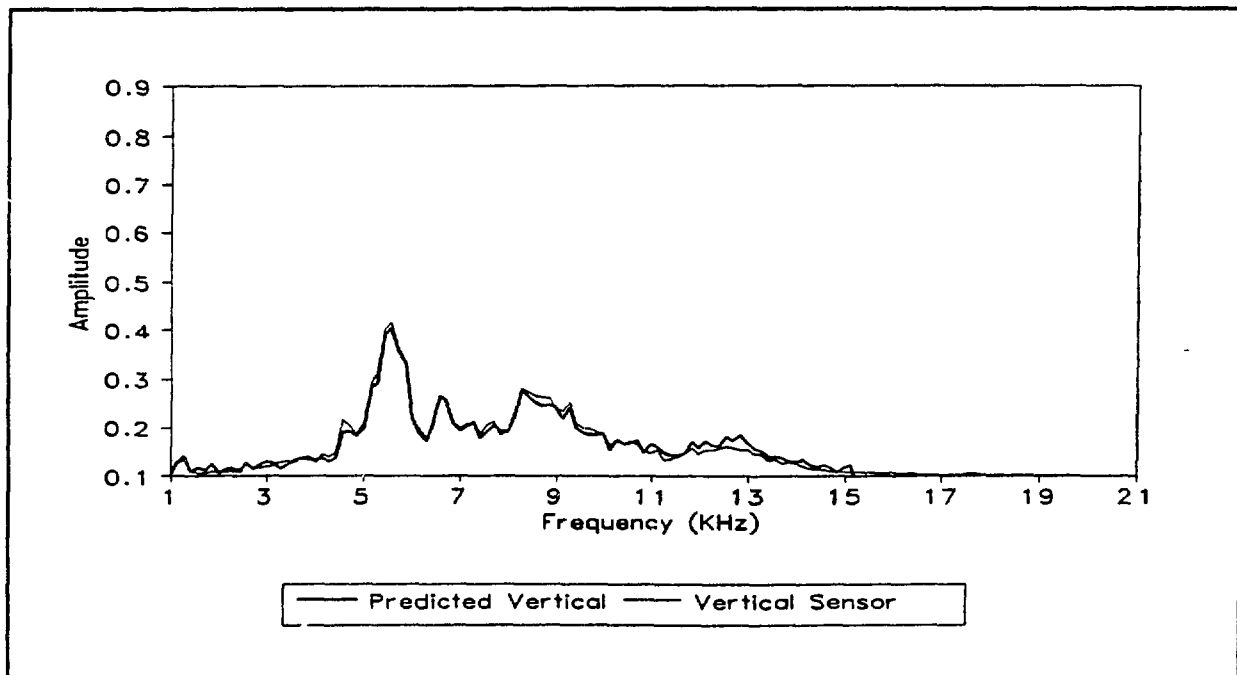
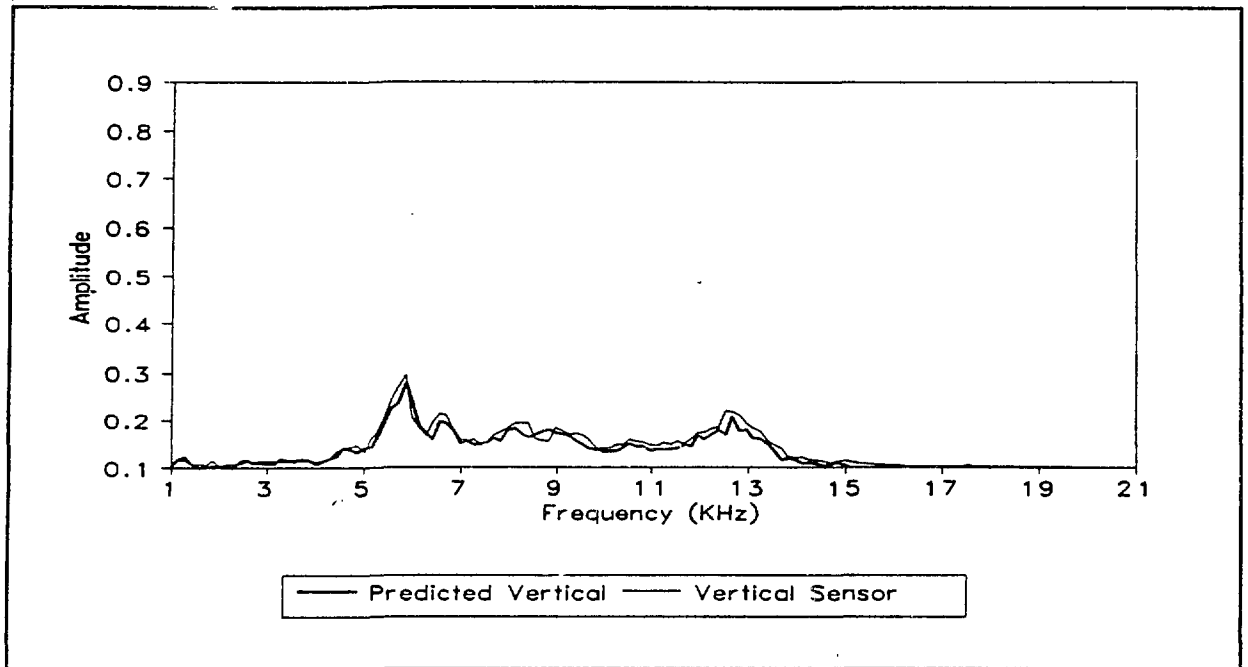
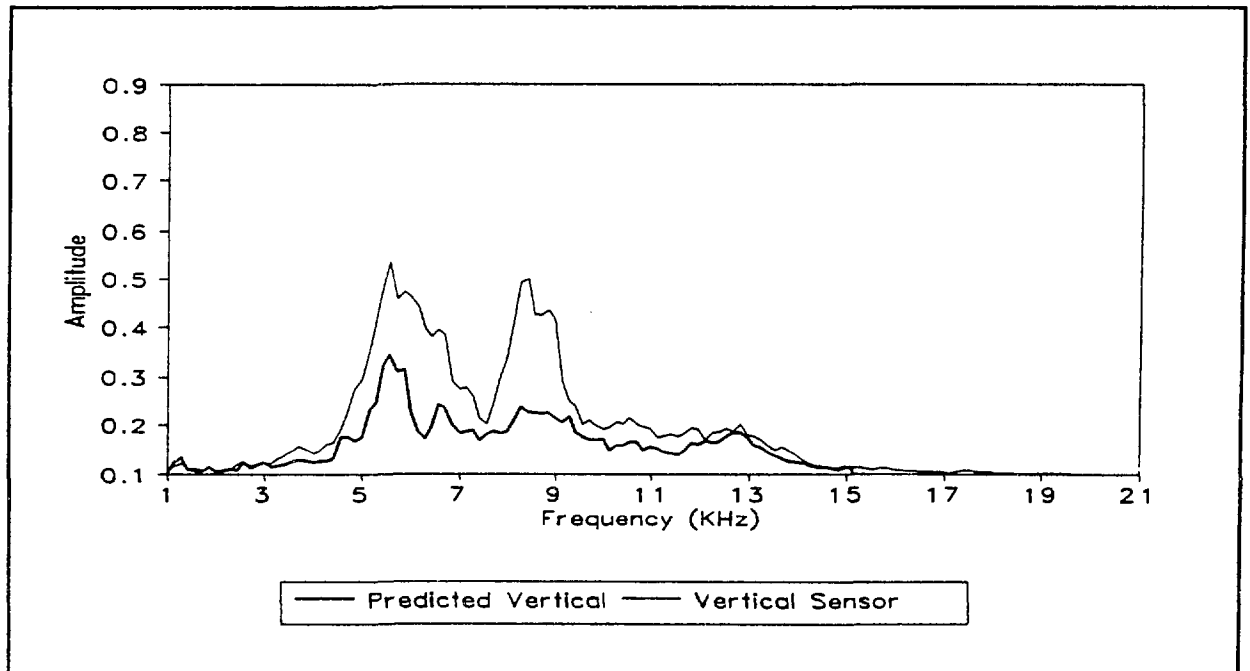


Figure 4. Predicted and Actual Spectra for Signature 2  
(Normal signature included in the training set)



**Figure 5. Predicted and Actual Spectra for Signature 5  
(Normal signature not included in the training set)**



**Figure 6. Predicted and Actual Spectra for Signature 7  
(Fault begins to develop)**

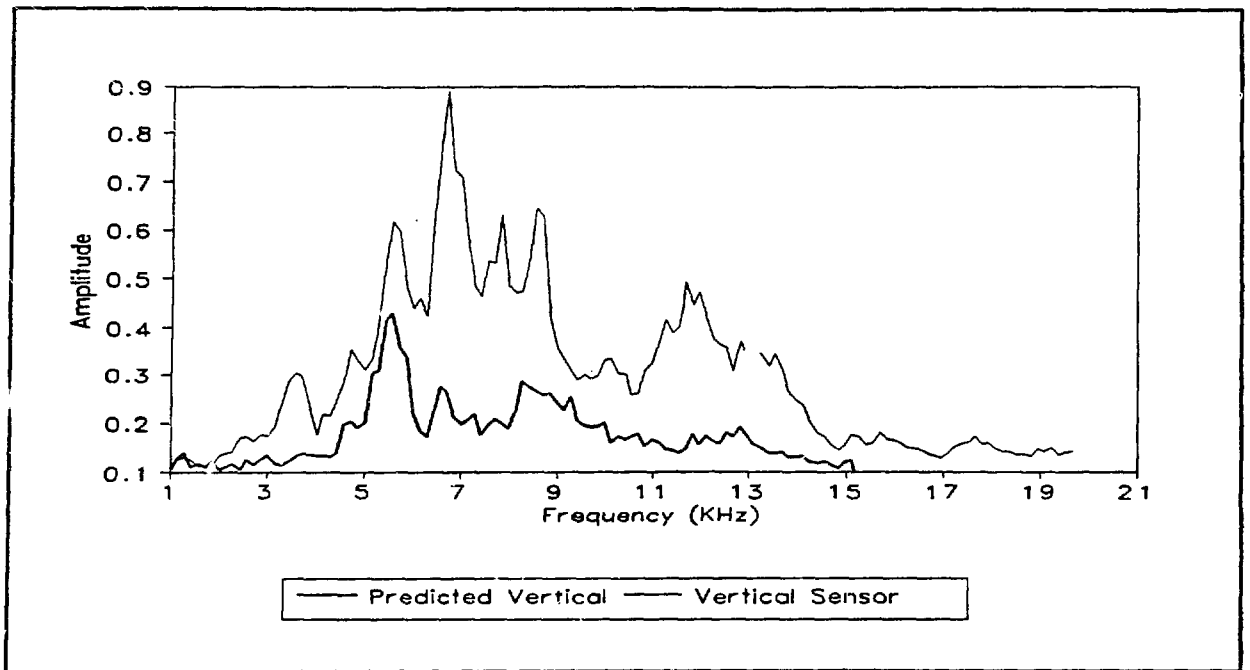


**Figure 7. Predicted and Actual Spectra for Signature 12 (Out-of-order bearing)**

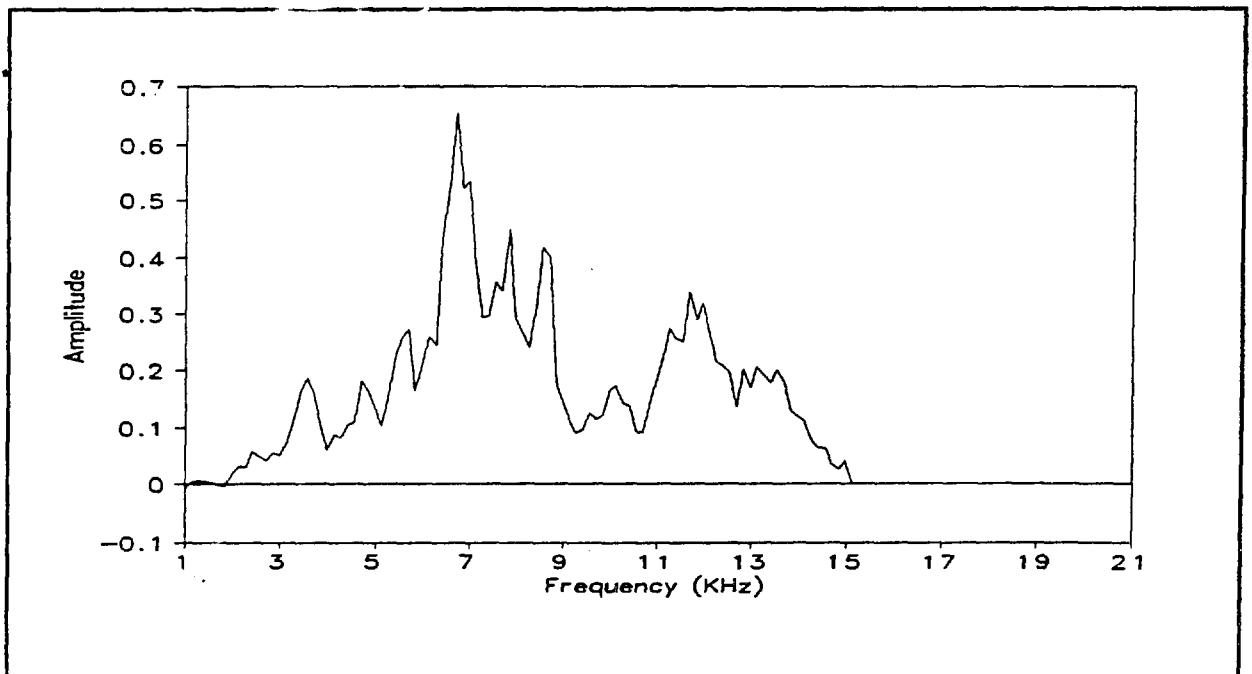


**Figure 8. Per-Frequency Descriptor for Signature 12**